BUILDING A STATE-SPACE MODEL TO PREDICT THE 3-D TEMPERATURE AND HUMIDITY DISTRIBUTION IN A VENTILATED TEST ROOM

JANSSENS K. [1,2], BERCKMANS D. [1] AND GOEDSEELS V. [1]

[1] Laboratory for Agricultural Buildings Research
K.U.Leuven, K. Mercierlaan 92,
B-3001 Heverlee, Belgium
[2] National Fund for Scientific Research, Belgium

ABSTRACT

In a mechanically ventilated room the indoor air is never perfectly mixed and considerable 3-D gradients of temperature and humidity often occur. An optimal control of the 3-D temperature and humidity distribution is essential to many processes. Model based predictive control (MBPC) offers many possibilities to this. However, before MBPC can be applied, it is first required to have an appropriate dynamic mathematical model of the process to be controlled.

Therefore, a state-space model was developed and tested in a laboratory test room (3 x 2 x 1.5 m). The state-space model describes the dynamic response of the 3-D temperature and humidity distribution in the test room to variations of the ventilation rate as control input. The wall temperature of the room is included as an additional input variable. To estimate the model parameters, 48 identification experiments were carried out. The 'mean square error' was calculated to evaluate the accuracy of the model. The model was found to predict the dynamic response of the 3-D temperature and humidity distribution with an average accuracy of 0.1222 °C and 0.1745 $g_{water}/kg_{dry\ air}$ over the 48 experiments.

KEYWORDS: modelling, temperature and humidity distribution, air flow pattern

1. Introduction

In a mechanically ventilated room the indoor air is never perfectly mixed (Barber and Ogilvie 1982). Due to the imperfect mixing, considerable 3-D gradients of temperature and humidity often occur.

Model based predictive control (MBPC) offers many possibilities to realise an optimal control of the 3-D temperature and humidity distribution in a ventilated room. MBPC is the most advanced control technique and has been found to be very succesfull in many applications, especially in the process industry (Van den Boom 1996). An important difference with the more classical P-, PI- and PID-controllers is the explicit use of a 'dynamic mathematical model of the process to be controlled'. This aspect is both the advantage and the disadvantage of MBPC. The advantage is that the behaviour of the MBPC-controller can be studied in detail and simulations can be made. The disadvantage is that a detailed study of the process behaviour has to be done before the actual MBPC-design can be started. About 80 percent of the work to be

done, is the dynamic modelling of the process to be controlled (Richalet 1993).

2. Objective

The main objective of this study is to develop and test a dynamic mathematical model that can be used as a basis for a model based predictive control (MBPC) of the 3-D temperature and humidity distribution in a mechanically ventilated room.

3. Method

3.1. Test room

The study was carried out in a laboratory test room with a total volume of 9 m³ (length = 3 m, width = 1.5 m, height = 2 m). The test room is shown in figure 1. Eight temperature sensors are distributed over the 4 walls to measure the dynamic behaviour of the wall temperature. A second envelope (7 in figure 1) is built around the test room to reduce the disturbing effects of varying laboratory conditions (opening doors,...). The total volume of the buffering interspace is 21 m³.

Five aluminium heating elements at low temperature (3 in figure 1) and an undeep hot water reservoir (4 in figure 1) are placed at the floor to simulate the heat and moisture production of the occupants. The total heat production of the 5 heating elements is 300 Watt. The temperature of the water in the reservoir is kept at 40 °C.

The ventilation rate can be controlled from 70 up to 300 m³/h. This results in rather high inlet velocities (0.49 m/s - 2.10 m/s) and high air exchange rates (7.8 - 33.3 refreshments per hour). The accuracy of the ventilation control is ± 6 m³/h.

The temperature and moisture content of the supply air are 11.5 °C and 6.5 g$_{water}$/kg$_{dry\ air}$. To visualise the air flow pattern, white smoke gasses are injected in the supply air.

In a previous study (Berckmans et al. 1993), the air flow pattern was visualised for different ventilation rates. Three categories of air flow patterns were found: horizontal (ventilation rate > 250 m³/h), unstable (ventilation rate = 250 m³/h) and falling (ventilation rate < 250 m³/h) air flow patterns. A digitised image of a falling and a horizontal air flow pattern is shown in the figures 2.1 and 2.2.

To measure the 3-D, time-varying gradients of temperature [°C] and absolute humidity [g$_{water}$/kg$_{dry\ air}$], 24 temperature and 24 humidity sensors are positioned in a 3-D grid (6 in figure 1). The temperature sensors are numbered from 1 to 24, while the humidity sensors are numbered from 25 to 48.

3.2. State-space model

A linear, discrete-time state-space model was developed to model the dynamic response of the 3-D temperature and humidity distribution in the test room to non-linear variations of the ventilation rate as control input. The wall temperature of the test room is included as an additional input variable. The structure of the state-space model is given in equation (1):

$$\underline{x}(k+1) = A.\underline{x}(k) + B.\underline{u}(k) \qquad (1)$$

$$\underline{y}(k) = C.\underline{x}(k) + D.\underline{u}(k)$$

in which

$$A = \begin{bmatrix} a_{11} & \cdots & 0 & 0 & \cdots & 0 \\ \vdots & \ddots & \vdots & \vdots & \ddots & \vdots \\ 0 & \cdots & a_{24\,24} & 0 & \cdots & 0 \\ 0 & \cdots & 0 & a_{25\,25} & \cdots & 0 \\ \vdots & \ddots & \vdots & \vdots & \ddots & \vdots \\ 0 & \cdots & 0 & 0 & \cdots & a_{48\,48} \end{bmatrix}$$
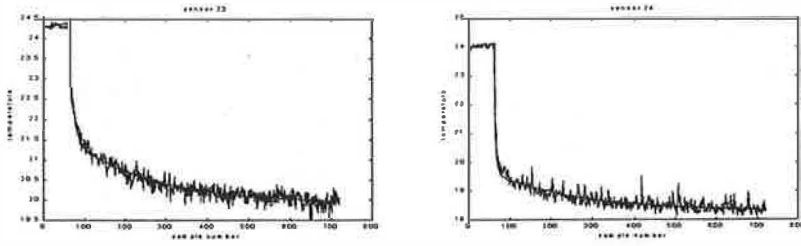
Figure 4: (1) measured and modelled dynamic response of temperature at sensor position 23 (TC_{23} = 98 s), (2) measured and modelled dynamic response of temperature at sensor position 24 (TC_{24} = 38 s).
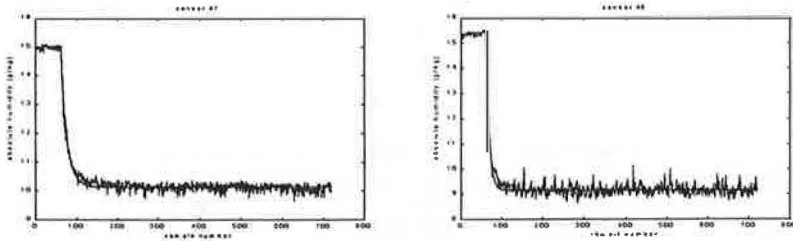

Figure 5: (1) measured and modelled dynamic response of absolute humidity at sensor position 47 (TC_{47} = 145 s), (2) measured and modelled dynamic response of absolute humidity at sensor position 48 (TC_{48} = 78 s).

experiment	ventilation rate [m3/h] before step	ventilation rate [m3/h] after step	air flow pattern in time-period after step	experiment	ventilation rate [m3/h] before step	ventilation rate [m3/h] after step	air flow pattern in time-period after step
exp140a	70	140	falling	exp220a	70	220	falling
exp140b	70	140	falling	exp220b	70	220	falling
exp140c	70	140	falling	exp220c	70	220	falling
exp150a	70	150	falling	exp230a	70	230	faling
exp150b	70	150	falling	exp230b	70	230	faling
exp150c	70	150	falling	exp230c	70	230	faling
exp160a	70	160	falling	exp240a	70	240	faling
exp160b	70	160	falling	exp240b	70	240	faling
exp160c	70	160	falling	exp240c	70	240	faling
exp170a	70	170	falling	exp260a	70	260	horizontal
exp170b	70	170	falling	exp260b	70	260	horizontal
exp170c	70	170	falling	exp260c	70	260	horizontal
exp180a	70	180	falling	exp270a	70	270	horizontal
exp180b	70	180	falling	exp270b	70	270	horizontal
exp180c	70	180	falling	exp270c	70	270	horizontal
exp190a	70	190	falling	exp280a	70	280	horizontal
exp190b	70	190	falling	exp280b	70	280	horizontal
exp190c	70	190	falling	exp280c	70	280	horizontal
exp200a	70	200	falling	exp290a	70	290	horizontal
exp200b	70	200	falling	exp290b	70	290	horizontal
exp200c	70	200	falling	exp290c	70	290	horizontal
exp210a	70	210	falling	exp300a	70	300	horizontal
exp210b	70	210	falling	exp300b	70	300	horizontal
exp210c	70	210	falling	exp300c	70	300	horizontal

Table 1: overview of the 48 step-up experiments.

sensor i	$mset_i$ [°C]	sensor i	$mset_i$ [°C]
1	0.1091	13	0.1226
2	0.1276	14	0.1333
3	0.0971	15	0.1073
4	0.1397	16	0.1976
5	0.0702	17	0.1057
6	0.1162	18	0.1802
7	0.1067	19	0.0905
8	0.1385	20	0.1918
9	0.0735	21	0.1289
10	0.1260	22	0.1349
11	0.0778	23	0.1049
12	0.1588	24	0.1266
		$mset_{av}$	0.1236

Table 2: the '$mset_i$ [°C]' for the temperature sensors 1 to 24.

sensor i	$mseh_i$ [g_{water}/$kg_{dry\ air}$]	sensor i	$mseh_i$ [g_{water}/$kg_{dry\ air}$]
25	0.1465	37	0.0967
26	0.1506	38	0.1313
27	0.1484	39	0.0940
28	0.1724	40	0.2160
29	0.2197	41	0.1853
30	0.3518	42	0.1502
31	0.1640	43	0.0908
32	0.1899	44	0.1125
33	0.1036	45	0.1094
34	0.1560	46	0.1193
35	0.0857	47	0.0961
36	0.1581	48	0.1150
		$mseh_{av}$	0.1485

Table 3: the '$mseh_i$ [g_{water}/$kg_{dry\ air}$]' for the humidity sensors 25 to 48.

experiment	$mset_{av}$ [°C]	$mseh_{av}$ [g_{water}/$kg_{dry\ air}$]	experiment	$mset_{av}$ [°C]	$mseh_{av}$ [g_{water}/$kg_{dry\ air}$]
exp140a	0.1061	0.1338	exp220a	0.1024	0.2001
exp140b	0.1016	0.1212	exp220b	0.1138	0.1489
exp140c	0.0996	0.1651	exp220c	0.1103	0.1245
exp150a	0.1113	0.1361	exp230a	0.1073	0.1677
exp150b	0.1126	0.1313	exp230b	0.1149	0.1961
exp150c	0.1109	0.1574	exp230c	0.1164	0.1782
exp160a	0.1205	0.1615	exp240a	0.1236	0.1485
exp160b	0.1173	0.1297	exp240b	0.1339	0.1540
exp160c	0.1165	0.1404	exp240c	0.1143	0.1328
exp170a	0.1239	0.1807	exp260a	0.1826	0.2521
exp170b	0.1171	0.1201	exp260b	0.1686	0.2582
exp170c	0.1154	0.1295	exp260c	0.1550	0.2348
exp180a	0.1203	0.1502	exp270a	0.1500	0.2019
exp180b	0.1134	0.1379	exp270b	0.1526	0.2217
exp180c	0.1140	0.1662	exp270c	0.1346	0.2304
exp190a	0.1005	0.1427	exp280a	0.1424	0.1826
exp190b	0.1131	0.1077	exp280b	0.1455	0.2345
exp190c	0.1086	0.1621	exp280c	0.1354	0.2350
exp200a	0.1091	0.1524	exp290a	0.1281	0.1931
exp200b	0.1114	0.1453	exp290b	0.1288	0.2335
exp200c	0.1057	0.1603	exp290c	0.1348	0.1983
exp210a	0.1188	0.1923	exp300a	0.1311	0.2370
exp210b	0.0986	0.1597	exp300b	0.1291	0.2397
exp210c	0.1108	0.1548	exp300c	0.1325	0.2354
			mean	0.1222	0.1745

Table 4: the '$mset_{av}$ [°C]' and '$mseh_{av}$ [g_{water}/$kg_{dry\ air}$]' for the 48 step-up experiments.

$$
B = \begin{bmatrix} b_{1,1} & b_{1,2} \\ \vdots & \vdots \\ b_{24,1} & b_{24,2} \\ b_{25,1} & 0 \\ \vdots & \vdots \\ b_{48,1} & 0 \end{bmatrix} \quad
C = \begin{bmatrix} 1 & \dots & 0 & 0 & \dots & 0 \\ \vdots & \ddots & \vdots & \vdots & \ddots & \vdots \\ 0 & \dots & 1 & 0 & \dots & 0 \\ 0 & \dots & 0 & 1 & \dots & 0 \\ \vdots & \ddots & \vdots & \vdots & \ddots & \vdots \\ 0 & \dots & 0 & 0 & \dots & 1 \end{bmatrix}
$$

$$
D = \begin{bmatrix} 0 & 0 \\ \vdots & \vdots \\ 0 & 0 \\ 0 & 0 \\ \vdots & \vdots \\ 0 & 0 \end{bmatrix} \quad
\underline{x}(k) = \begin{bmatrix} x_1(k) \\ \vdots \\ x_{24}(k) \\ x_{25}(k) \\ \vdots \\ x_{48}(k) \end{bmatrix}
$$

$$
\underline{Y}(k) = \begin{bmatrix} y_1(k) \\ \vdots \\ y_{24}(k) \\ y_{25}(k) \\ \vdots \\ y_{48}(k) \end{bmatrix} \quad
\underline{u}(k) = \begin{bmatrix} u_1(k) \\ u_2(k) \end{bmatrix}
$$

The vectors $\underline{u}(k)$ and $\underline{y}(k)$ contain the input and output data of the model: u_1 represents the ventilation rate [m³/h], u_2 the wall temperature [°C] of the test room (considered to be uniform), $y_1, y_2, \dots, y_{24}$ the temperature [°C] at the sensor positions 1 to 24 and $y_{25}, y_{26}, \dots, y_{48}$ the absolute humidity [$g_{water}/kg_{dry\ air}$] at the sensor positions 25 to 48. The steady-state levels are removed from the input and output data to enable the system identification. The matrices A and B contain the discrete-time parameters of the model. The system matrix A describes the dynamics of the process. The time constant of the first order dynamic response at the 48 sensor positions in the test room can be calculated from A. Therefore, equation (2)

is used, in which TC_i [s] is the time constant at sensor position i, Δt [s] the sampling rate and a_{ii} the i-th diagonal element of matrix A.

$$
TC_i = \frac{-\Delta t}{\ln(a_{ii})} \tag{2}
$$

3.3. Step-up experiments

In order to estimate the parameter matrices A and B, 48 step-up experiments were carried out. In these step-up experiments the ventilation rate (control input) was increased step-wise from 70 m³/h to 140, 150, 160, 170, 180, 190, 200, 210, 220, 230, 240, 260, 270, 280, 290 or 300 m³/h. The ventilation rate, the wall temperature, the temperature at the sensor positions 1 to 24 and the absolute humidity at the sensor positions 25 to 48 were measured with a time-step (Δt) of 10 seconds. The air flow pattern was visualised in the time-period after the step. The time-duration of the different step-up experiments was 2 hours or 720 time-samples. An overview of the 48 step-up experiments is given in table 1.

The 'least squares identification scheme' (Ljung 1987) was used to estimate the parameter matrices A and B.

The average mean square error of temperature '$mset_{av}$ [°C]' and the average mean square error of humidity '$mseh_{av}$ [$g_{water}/kg_{dry\ air}$]' were calculated to compare the modelled with the measured 3-D temperature and humidity distribution. The average mean square error of temperature '$mset_{av}$' is defined in the equations (3) and (4), in which '$mset_i$' is the mean square error of temperature at sensor position i and $y_i(k)_{mod}$ and $y_i(k)_{meas}$ the modelled and measured temperature at sensor position i and at time-step k. The average mean square error of humidity '$mseh_{av}$' is defined in the equations (5) and (6), in which '$mseh_i$' is the mean square error of humidity at sensor position i and $y_i(k)_{mod}$ and $y_i(k)_{meas}$ the modelled and measured absolute humidity at sensor position i and at time-step k.

305

$$mset_{av} = \frac{\sum\limits_{i=1}^{24} mset_i}{24} \qquad (3)$$

$$mset_i = \frac{\sum\limits_{k=1}^{720} |y_i(k)_{meas} - y_i(k)_{mod}|}{720} \qquad (4)$$

$$mseh_{av} = \frac{\sum\limits_{i=25}^{48} mseh_i}{24} \qquad (5)$$

$$mseh_i = \frac{\sum\limits_{k=1}^{720} |y_i(k)_{meas} - y_i(k)_{mod}|}{720} \qquad (6)$$

4. Results and discussion

4.1. Step-up experiment 'exp240a'

Step-up experiment 'exp240a' is selected as a representative example to show and discuss some basic results of the model. The measured step-increase of the ventilation rate (from 70 to 240 m³/h) and the measured dynamic behaviour of the wall temperature are shown in the figures 3.1 and 3.2. The estimated parameter matrices A and B are given below:

$$A = \begin{bmatrix} 0.8476 & \dots & 0 & 0 & \dots & 0 \\ \vdots & \ddots & \vdots & \vdots & \ddots & \vdots \\ 0 & \dots & 0.738 & 0 & \dots & 0 \\ 0 & \dots & 0 & 0.9482 & \dots & 0 \\ \vdots & \ddots & \vdots & \vdots & \ddots & \vdots \\ 0 & \dots & 0 & 0 & \dots & 0.8727 \end{bmatrix}$$

$$B = \begin{bmatrix} -0.0026 & 0.1003 \\ \vdots & \vdots \\ -0.0065 & 0.1387 \\ -0.0012 & 0 \\ \vdots & \vdots \\ -0.0044 & 0 \end{bmatrix}$$

The matrices A and B indicate that the temperature at the sensor positions 1 to 24 (y_1, y_2,… ,y_{24}) shows a first order response to the ventilation rate and the wall temperature as input variables. The matrices A and B also shows that the dynamic response of temperature is different at the 24 sensor positions in the test room. The figures 4.1 and 4.2 illustrate this for the sensors 23 and 24. The time constant TC_{23} is 98 seconds, while TC_{24} is 38 seconds. The different dynamic response is due to the imperfect mixing of the indoor air.

In this process of imperfect mixing the air flow pattern is of crucial importance. After the ventilation step, the supply air is falling down towards the floor and is then forced through the floor area until it reaches the opposite wall. There, a part of the air moves upward along the wall and recirculates through the ceiling area. This creates a large counter-clockwise vortex. Due to this air circulation, sensor 24 (in floor area) responds rather fast (TC_{24} = 38 seconds) to the step-increase of the ventilation rate, while sensor 23 (in ceiling area) shows a rather slow response (TC_{23} = 98 seconds).

It can also be seen from the matrices A and B that the absolute humidity at the sensor positions 25 to 48 (y_{25}, y_{26},… ,y_{48}) shows a first order response to the step-increase of the ventilation rate, but not to the wall temperature of the test room ($b_{25.2}$, $b_{26.2}$,…, $b_{48.2}$ = 0). This is the main point of difference with the dynamic temperature response. Due to the imperfect mixing of the indoor air, there is also a different dynamic response of absolute humidity at the different sensor

positions in the test room. The figures 5.1 and 5.2 illustrate this for the humidity sensors 47 and 48. Due to the counter-clockwise vortex of air flow, sensor 48 (in floor area) responds rather fast (TC_{48} = 78 seconds) to the ventilation step, while sensor 47 (in ceiling area) shows a rather slow response (TC_{47} = 145 seconds).

In table 2 an overview is given of the calculated 'mset$_i$' (equation 4) for the temperature sensors 1 to 24. The minimum value, the maximum value, the mean value and the standard deviation are 0.0702, 0.1976, 0.1236 and 0.0337 °C. In table 3 an overview is given of the calculated 'mseh$_i$' (equation 6) for the humidity sensors 25 to 48. The minimum value, the maximum value, the mean value and the standard deviation are 0.0857, 0.3518, 0.1485 and 0.0582 gwater/kgdry air.

4.2. The 48 step-up experiments

The above analysis was done for the 48 step-up experiments. Similar results were found. In table 4 an overview is given of the calculated 'mset$_{av}$' (equation 3) and 'mseh$_{av}$' (equation 5) for the 48 step-up experiments. It can be concluded from the table that the dynamic response of the 3-D temperature and humidity distribution is modelled with an average accuracy of 0.1222 °C and 0.1745 gwater/kgdry air over the 48 step-up experiments.

5. Conclusions

1. A state-space model was developed to model the dynamic response of the 3-D temperature and humidity distribution in a laboratory test room (3 x 2 x 1.5 m) to variations of the ventilation rate as control input. The wall temperature of the test room is taken into account as an additional input variable. The parameters of the model were estimated from 48 step-up experiments.

2. Due to the imperfect air mixing, the dynamic response of temperature and absolute humidity varies in space.

3. The state-space model was found to predict the dynamic response of the 3-D temperature and humidity distribution with an average accuracy of 0.1222 °C and 0.1745 gwater/kgdry air over the 48 step-up experiments.

6. References

Barber E.M. and Ogilvie J.R., 1982. Incomplete mixing in ventilated air spaces. Part 1: theoretical considerations. Can. Agric. Engng., Vol. 24, p. 25-29.

Berckmans D., De Moor M., Van De Weyer K., 1993. Visualisation and quantification of the air flow pattern in ventilated spaces by using image analysis. ASAE International Winter Meeting, Chicago, Illinois, USA, Dec. 14-17, 1993, ASAE-paper No. 934575.

Ljung L., 1987. System identification: theory for the user. Prentice Hall, Englewood Cliffs, New Jersey, pp. 519.

Richalet J., 1993. Industrial applications of model based predictive control. Automatica, 29(5), p. 1251-1274.

Van den Boom T.J.J., 1996. Model based predictive control: status and perspectives. Proceedings of CESA'96 IMACS Multiconference: Symposium on control, optimization and supervision, Lille, France, July 9-12, 1996, Vol. 1, p. 1-12.
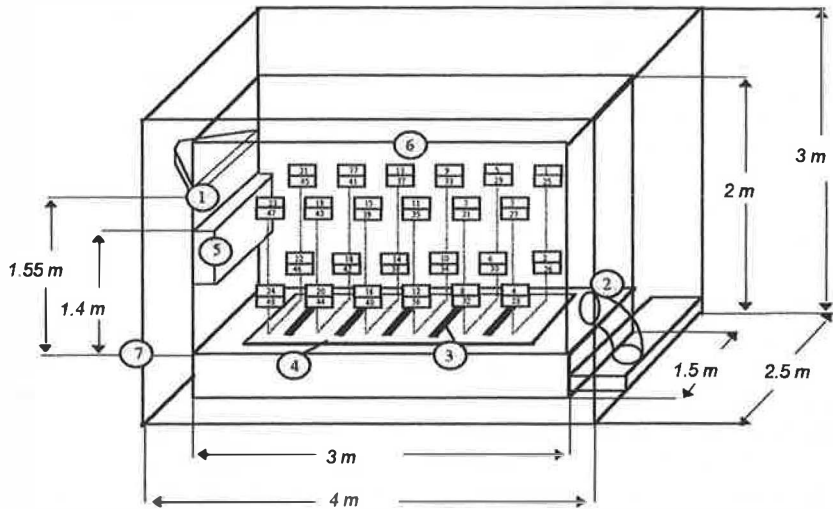
Figure 1: laboratory test room: **1.** air inlet, **2.** air outlet, **3.** aluminium heating element at low temperature, **4.** undeep hot water reservoir, **5.** extra heating element, not used in this study, **6.** 3-D sensor grid, **7.** second transparent envelope.
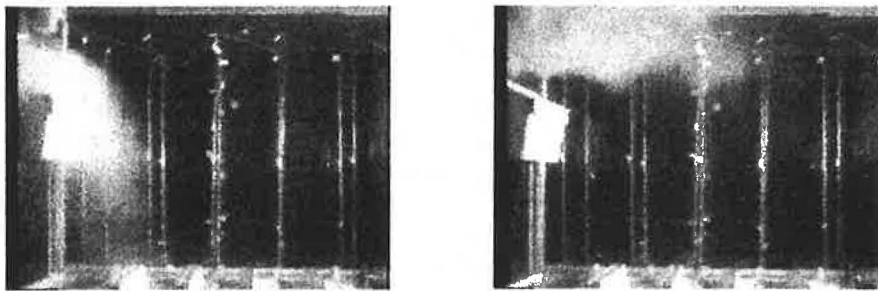

Figure 2: (1) falling air flow pattern, (2) horizontal air flow pattern.

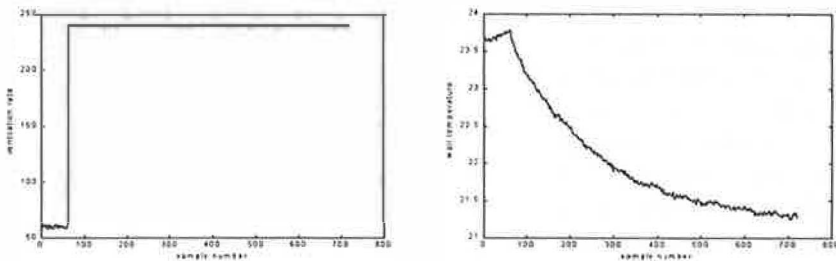**Figure 3:** (1) measured ventilation rate [m^3/h] and (2) measured wall temperature [°C].

308